Building, Optimizing, and Maintaining a Xenon Cold-Trap Sampling System

Jon Balajthy

Abstract

1 Introduction

For almost 40 years, xenon has been used as a detector medium in radiation detectors.

2 Technical Overview

A cold trap sampling system is designed to flow a sample of xenon with trace amounts of impurities through a section of liquid nitrogen cooled plumbing, to a mass-spectrometer for purity analysis. This document will deal particularly with krypton, but the method described also works for most simple impurities such as helium, argon, nitrogen, oxygen, methane, etc.. Less volatile impurities such as water and large hydrocarbons tend to freeze along with the xenon, so are not detected.

The operating principle is similar the that of freeze distillation. The bulk xenon is frozen to the cold plumbing leaving only the xenon ice vapor pressure at the output of the cold-trap. The flow of krypton is left largely unaffected. The resulting mixture which exits the cold-trap can be up up to 10^9 times enriched in krypton. A cold-trap used in conjunction with a residual gas analyzer (RGA) whose sensitivity is about one part in 10^6, is able to measure concentrations of krypton in a xenon sample down to the order of one part in 10^{15}.

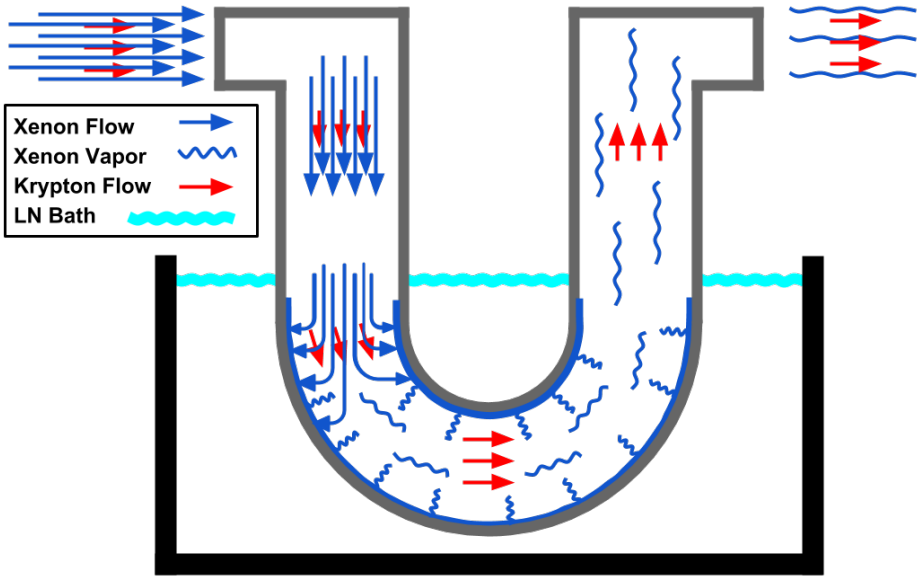

Figure 1: Cartoon version of what happens during a cold trap analysis.

2.1 System Construction

A cold trap sampling system should be laid out as described by figure 9. There will likely be additional transfer lines needed for collecting samples, recovering xenon, etc., but figure 9 fully describes the plumbing necessary to analyze a sample of xenon.

The system should have 100% metal-seals such as VCR or CF. Elastomer internals have the potential to become contaminated with krypton and destroy the sensitivity of the system and so should be limited.Traditionally, hardware used for this type of system is as follows:

- The plumbing should be entirely composed of UHP stainless steel.
- The sample bottle, SB, is a 1 gallon Swagelok DOT compliant sample cylinder.
- The valves, V1 through V7 are some type of high purity shutoff valve. For automated systems, the Swagelok DF series diaphragm valves with pneumatic actuators are used.

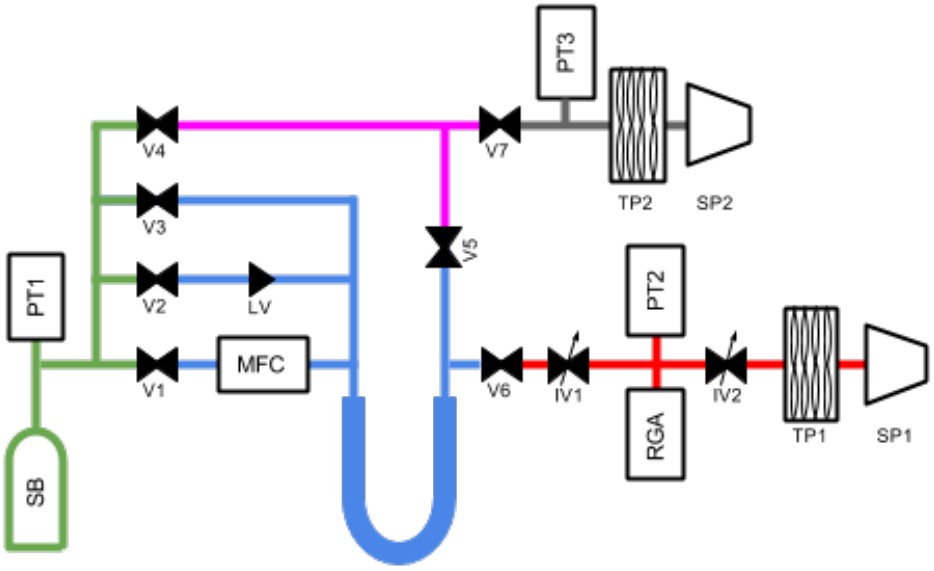

Figure 2: Plumbing diagram of a general purpose cold-trap sampling system. The green section is referred to as the sample volume, the blue section is the cold trap volume, and the red section is the RGA volume. These are the sections used during analysis of a xenon sample. The pink section is the bypass line which serves two purposes. It is used to relieve pressure in the cold trap while the system is warming and acts as the access line to the pump-out turbo pump, TP2.

When possible, it is better to use the Swagelok B series bellows valves with the spherical copper stem tip option, since the DF series has a polymer seat, however these are more difficult to automate.

- The sample pressure transducer is a capacitance manometer such as the MKS Baratron with a full scale of at least 3,000 Torr.

- The leak valve, LV, is a metering valve.

- The mass flow controller, MFC, should be metal sealed, and have a full range of about 10 SLM. The Celerity UNIT1660 is a good example. Although no longer in production,

they are fairly easy to find used.

- The cold trap itself is some UHP stainless steel plumbing that is bent or welded into a shape that allows it to be submerged in a liquid nitrogen bath. Currently, the optimal cold-trap geometry is a 1/2 inch "stocking" trap, as described in section 6.4.

- Traditionally IV1 has been a Swagelok B series bellows valves with the spherical copper stem tip option, however it's likely that the regulating stem tip would be better suited to the task.

- PT2 and PT3 are any cold cathode or inverted magnetron gauge that have an operating range of at least 10^{-8} to 10^{-4} Torr.

- The residual gas analyzer, RGA, is the SRS RGA200.

- IV2 needs to have a significantly lower impedance than IV1, so some type of 2.75" CF sealed all-metal vacuum valve should be used. A Varian UHV right angle valve, part No. 9515027 has been used in the past with good results.

- TP1 and TP2 are turbo-molecular pumps with pumping speed of at least 70 liters per second. The Varian V70, V81, and V84 have all been used with good results.

- SP1 and SP2 are the backing pumps for TP1 and TP2. They should be at least equivalent to the Agilent model SH110 scroll pump.

2.2 Operational Outline

The exact steps required for a particular analysis can be quite complex, and some detailed example procedures can be found in appendix A. A general outline of the operation of a cold trap sampling system is as follows:

1. A xenon sample is collected and stored in the sample volume until the beginning of analysis.

2. The system begins with all the valves closed.

3. The cold trap is immersed in a liquid nitrogen bath, and base layer of xenon ice is formed.

4. Baseline pressures are measured by the RGA by opening V6, exposing the RGA volume the the xenon ice vapor pressure present in the cold trap volume. Usually these baselines are established over a period of ten or more minutes.

5. Leaving V6 open, V1 or V2 is opened, allowing the xenon sample to freeze into the cold trap at a controlled flow rate. This will usually takes several minutes.

As described in figure 1, the xenon pressure at the RGA will remain constant during this step, but there will be a flow of krypton at the output of the cold-trap which will cause a rise in the krypton partial pressure in the RGA volume. It is this partial pressure pressure rise that will be analyzed to give the concentration of krypton in the xenon sample.

6. After the sample volume has been exhausted, V1(2) will be closed, and the krypton partial pressure is allowed fall back to its prior value.

At this point, the purity analysis of the xenon sample has been completed, but the system is not in a safe state. Only a microscopic amount of xenon has been pumped out through TP1, so the full mass of the xenon sample is frozen in the cold trap. If this is allowed to vaporize without proper precautions, the RGA and TP1 could be damaged by over-pressure. It is therefore extremely important to isolate the RGA volume from the cold-trap volume before allowing the cold-trap to rise above liquid-nitrogen.

7. Close V6.

If the sample mass was large enough, there could be enough xenon ice in the cold trap to damage the system instrumentation or even cause the plumbing system to rupture once it warms to the gas phase. This is why it is important to have rupture disks installed on the cold trap. To avoid damage to the system, the cold trap volume should be vented to the sample volume. Valve V3 provides a path from the input of the cold trap to the sample volume without the added impedance of the MFC or LV.

8. Open V3.

This is where the bypass line comes in. With a cold-trap made from 1/2" plumbing, it is likely that an ice blockage will form once the xenon flow has stopped. This ice blockage could cause a dangerous pressure differential between the input and output of the trap. By opening the bypass line, the output of the cold trap has a second path to the sample volume.

9. Open V4 and V5.

The system is now in a safe state and the cold trap can be allowed to warm back to room temperature. The remaining xenon can then be recovered or discarded as desired, after which the system should be pumped to vacuum before collecting the next sample. It is important to note that this pump-out should be done using TP2, since the RGA volume should be kept at vacuum except for maintenance. The bypass line, as configured, allows the cold-trap volume and sample volume to be pumped out independent of one another.

3 Idealized Cold Trap Response

In order to optimize the sensitivity of the cold-trap system, it is good to have an understanding of the basics of vacuum physics. A vacuum system can be analogized to an electrical circuit, with pressure taking the place of voltage, flow rate (Q) taking the place of current, and impedance

(Z) taking the place if resistance. This analogy gives us with the equation:

$$\Delta P = Q \cdot Z \tag{1}$$

Here, it is useful to define a new quantity, S, which is called the "volumetric flow rate" or "pumping speed". S is defined:

$$S \equiv Av = \frac{dV}{dt} = Q/P, \tag{2}$$

where A is the cross-sectional area of the pipe, and v is the flow velocity, and dV is the volume of gas which passes a point in the system in time dt. An effective pumping speed can be calculated for any point in the vacuum system through the equation:

$$1/S_{eff} = 1/S_p + Z_{total}, \tag{3}$$

where S_p is the speed of the pump which is acting on the system, and Z_{total} is the total impedance between the pump and the specified point in the system. We can then calculate the steady-state pressure at any point in the system (*1*):

$$P = Q/S_{eff}. \tag{4}$$

3.1 Vacuum Impedances

The calculation of system impedances depends on which flow regime a gas resides. The flow regime is determined by whether a given gas molecule interacts primarily with other molecules, or with the walls of the vacuum chamber. The flow regime can be characterized by the Knudsen number, $K \equiv \lambda/d$, where λ is the mean free path, and d is the inner diameter of the vacuum chamber. For $K >> 1$, a gas molecule is very likely to encounter the wall of the system before encountering another gas molecule; this is the molecular flow regime. When $K << 1$, the system is in the viscous flow regime where a gas molecule will be interacting predominantly

with other gas molecules. If K is $O(1)$, the system is in what is referred to as the intermediate regime. (*1*)

In the molecular flow regime the impedance of a system element will depend on the geometry of the element, and on the molecular weight and temperature of the gas in question, but it will not depend on the pressure of that gas. For instance, the impedance of an aperture with area A will be given by: (*1*)

$$Z = \sqrt{\frac{2\pi M}{8kTA^2}}. \tag{5}$$

In the intermediate regime, the impedance picks up a complicated pressure dependance that can not be exactly calculated. Xenon gas inside the cold trap is at 1.8×10^{-3} Torr and 77 Kelvin. (*2*) In a 0.5" diameter cold trap the xenon has a Knudsen number of 0.6. This puts this section of plumbing in the intermediate gas flow regime rather than the molecular flow regime, and limits the accuracy of any results calculated using the molecular flow approximation. The role of vacuum equations in this document is to provide qualitative predicts on how the krypton pressure at the RGA will behave in response to changes in system parameters. The exact response of the system is always characterized empirically, as will be described in section **??**. For this purpose, the molecular flow approximation will suffice to motivate and direct our empirical investigations. (*1*)

The particular impedances of interest here are impedance between the cold-trap and the RGA (Z_1) and the impedance between the RGA and TP1 (Z_2). IV1 and IV2 are in place so that Z_1 and Z_2 can be fine tuned to an optimal arrangement. This optimization will be described further in section **??**, but first there is a hard constraint that must be placed on the relative values of Z_1 and Z_2.

The RGA has a maximum operating pressure of 1×10^{-6} Torr, although we have found that operating at about 1×10^{-5} Torr is possible with minimal degradation of the CDEM. When analyzing xenon samples with a concentration of about one part per million or less, the xenon

partial pressure, PP_{Xe}, will dominate the absolute pressure at the RGA. PP_{Xe} is the sourced by the vapor of the xenon ice in the cold trap, which is $P_{ICE} = 1.8 \times 10^{-3}$ Torr, and so needs to be reduced by a factor of about 100 or more between the cold-trap and the RGA (*2*).

There are several compounding factors that come into play when deciding exactly what PP_{Xe} should be. These will be discussed in later sections, so we will take it as given here that the sensitivity is optimized between $PP_{Xe} = 5 \times 10^{-6}$ Torr, and $PP_{Xe} = 2 \times 10^{-5}$ Torr, and is largely unaffected by deviations within this range. For the sake of simplicity, we will usually demand that PP_{Xe} to be the default pressure that the system plumbing gives when IV1 and IV2 are maximized. For the system described above, the this pressure will be about 1×10^{-5} Torr.

Returning to the vacuum equations we will see that although we have artificially defined PP_{Xe}, Z_1 and Z_2 are not fully determined by this choice. By using equations 1 and 4, and the requirement that $PP_{Xe} = 1 \times 10^{-5}$ Torr, we place a constraint on the impedances:

$$Q_{Xe,RGA} = PP_{Xe} S_{RGA} = \frac{P_{ICE} - PP_{Xe}}{Z_1} \approx \frac{P_{ICE}}{Z_1}, \tag{6}$$

where $1/S_{RGA} = 1/S_{TP1} + Z_2$. This gives,

$$S_{RGA} \cdot Z_1 = \frac{P_{ICE}}{PP_{Xe}} = 180. \tag{7}$$

S_{RGA} is usually dominated by Z_2. Depending on the model of pump used, the speed of the turbo pump for xenon is around 50 liters per second. The impedance of cylindrical plumbing with a diameter of 1.5 inches is about $\frac{1}{320} s/L$ per centimeter of plumbing. (*1*) In a typical system there will be the equivalent of about 5 feet of plumbing between the RGA and TP1, so the nominal value of Z_2 will be roughly 0.48 seconds per liters for xenon, indicating a maximum S_{RGA} of 2.1 liters per second. (*1*) This means the fully-open value of Z_1 should be about 85 seconds per liter for xenon. The exact numerical value of S_{RGA} and Z_1 are largely unimportant, and when optimizing the system impedances as described in section **??**, we will work in units relative to the fully open state, rather than liters per second.

3.2 Generalized Cold Trap System Response

The operating principle of cold-trap sampling is that while the xenon gets frozen into the cold-trap, the trace gasses, such as krypton pass through. Another way to put this is that at the output of the cold trap the xenon is frozen to a constant pressure, while krypton mass flow is conserved. In practice, the conservation is not perfect, so we add a throughput constant, $\alpha \equiv Q_{Kr,RGA}/Q_{Kr,CT}$, where $Q_{Kr,CT}$ is the flow rate into the cold trap, and $Q_{Kr,RGA}$ is the equilibrium flow rate of krypton out of the trap, and the flow rate of xenon into the cold-trap ($Q_{Xe,CT}$) is constant. $Q_{Kr,CT}$ is equal to $Q_{Xe,CT}$ times the concentration of krypton in the xenon sample, Φ_{Kr}. These relations put together, give us the following equation:

$$Q_{Kr,RGA} = \alpha Q_{Xe,CT} \Phi_{Kr}. \tag{8}$$

Plugging this into the vacuum equations, we can find the relationship between the parameter of interest, Φ_{Kr}, and the measurable quantities, Q_{Xe_0} and $PP_{Kr,eq}$:

$$PP_{Kr,eq} = \frac{\alpha}{S_{RGA}} Q_{Xe,CT} \Phi_{Kr}. \tag{9}$$

This relation shows the proportionality between partial pressure, and flow-rate times concentration that was found experimentally in (*3*) and (*4*). By imposing the constraint from equation 7 we can see how altering the system impedance is expected to affect $PP_{Kr,eq}$, the equilibrium pressure of krypton at the RGA:

$$PP_{Kr,eq} = \frac{\alpha}{180} Z_1 Q_{Xe,CT} \Phi_{Kr}. \tag{10}$$

From the vacuum equations, we can also find the expected response of the system to an impulse of krypton. To do so, we would like to make the assumption that the RGA volume and the cold trap volume have a vanishingly small internal impedance, which means that the pressure at the input is equal to the pressure at the output. This is reasonable for the RGA

volume which is constructed of 1.5 inch plumbing. However, we find that the bends in the cold trap plumbing cause this approximation to break down in when the xenon ice extends past the first leg of the trap. The effects of this breakdown will be discussed in a later section, but for now we will remain in the limit of small xenon flow rate and small xenon sample size where the approximation does provide largely valid predictions.

In a volume with no internal impedance, the amount of krypton contained by that volume is defined as $P_{Kr}V$. If the volume is being evacuated at a constant volumetric rate, S, while at the same time being sourced by some time-dependent flow rate, $Q(t)$ the amount of krypton will change according to the equation:

$$V\frac{dP_{Kr}}{dt} = Q(t) - SP_{Kr}. \tag{11}$$

The response of $P_{Kr}(t)$ to an impulse of flow, $Q(t) = P_0V\delta(t)$ is then:

$$P_{Kr}(t > 0) = P_0e^{-t/\tau}, \tag{12}$$

where $\tau = V/S$. The time dependent $P_{Kr}(t)$ can then be found by convolving $Q(t)$ with this impulse response.

Applying this impulse response to the RGA volume (V_{RGA}) and cold trap volume (V_{CT}), we can find an expected time dependence of the krypton RGA pressure, $P_{Kr,RGA}(t)$. The flow rate into the RGA volume is equal to the flow rate out of the cold trap volume, so it is given by:

$$Q_{Kr,RGA}(t) = \frac{P_{Kr,CT}(t)}{Z_1 + 1/S_{RGA}} \approx P_{Kr,CT}(t)/Z_1, \tag{13}$$

where $P_{Kr,CT}(t)$ is the time-dependent pressure of krypton in the cold trap volume. So to calculate the expected $P_{Kr,RGA}(t)$, we must first calculate $P_{Kr,CT}(t)$. This can be done by convolving the the known flow of krypton into the trap, $Q_{Kr,CT} = \Phi Q_{Xe,CT}(t)$, with the impulse response of the cold trap volume. We can then convolve the resulting $Q_{Kr,RGA}(t)$ with the response of the RGA volume to predict the overall response of the system to the input flow rate.

The response time for the cold trap volume will be given by:

$$\tau_{CT} = V_{CT}\frac{1}{Z_1 + 1/S_{RGA}} \approx V_{CT}Z_1, \tag{14}$$

and the response time for the RGA volume will be given by:

$$\tau_{RGA} = V_{RGA}/S_{RGA}. \tag{15}$$

The condition $Z_1 S_{RGA} = 180$ from equation 7, combined with the fact that in a typical system, $V_{RGA} \approx V_{CT}$, means that the RGA volume is expected to respond much more quickly than the cold trap volume. Therefore the overall response of the system will be dominated by the response of the cold trap, and the shape of $P_{Kr,RGA}$ will be well approximated by the shape of $P_{Kr,CT}$.

In this document we use flow rate profiles for xenon of the form:

$$Q_{Xe,CT}(t) = \begin{cases} Q_0 & \text{for } \leq t \leq T \\ 0 & \text{otherwise} \end{cases} \tag{16}$$

If $Q_{Xe,CT}(t)$ is given by equation 16, the instantaneous krypton pressure in the cold trap will be given by:

$$\frac{P_{Kr,CT}(t)}{\Phi Q_0 Z_1} = \begin{cases} 0 & \text{for } t < 0 \\ 1 - e^{-\frac{t}{\tau_{CT}}} & \text{for } 0 \leq t \leq T \\ (1 - e^{-\frac{T}{\tau_{CT}}})e^{-\frac{t-T}{\tau_{CT}}} & \text{for } t > T \end{cases} \tag{17}$$

Applying the response of the RGA volume gives the result:

$$\frac{P_{Kr,RGA}(t)}{\Phi Q_0/S_{RGA}} = \begin{cases} 0 & \text{for } t < 0 \\ 1 - e^{-\frac{t}{\tau_{RGA}}} - \frac{e^{-\frac{t}{\tau_{CT}}} - e^{-\frac{t}{\tau_{RGA}}}}{1-\tau_{RGA}/\tau_{CT}} & \text{for } 0 \leq t \leq T \\ e^{-\frac{t-T}{\tau_{RGA}}}(1 - e^{-\frac{T}{\tau_{RGA}}} - \frac{e^{-\frac{T}{\tau_{CT}}} - e^{-\frac{T}{\tau_{RGA}}}}{1-\tau_{RGA}/\tau_{CT}})... & \\ +\frac{e^{\frac{T}{\tau_{CT}}}-1}{1-\tau_{RGA}/\tau_{CT}}(e^{-\frac{t}{\tau_{CT}}} - e^{-\frac{t}{\tau_{RGA}}+T(1/\tau_{RGA}-1/\tau_{CT})}) & \text{for } t > T \end{cases} \tag{18}$$

Note that in the limit $\tau_{RGA} << \tau_{CT}$, the right side of equation 18 reduces to the right side of equation 17.

Equation 17 does a good job in predicting the shape of $P_{Kr,RGA}$ when Q_0 and Z_1 are small as seen in figure 3. A fit to equation 17 produces a best fit time constant of 12.2 seconds. The volume of the cold trap used for this trace is 183.8 cc, which would point to $Z_1 = 66.7$ seconds per liter and $S_{RGA} = 2.70$ liters per second.

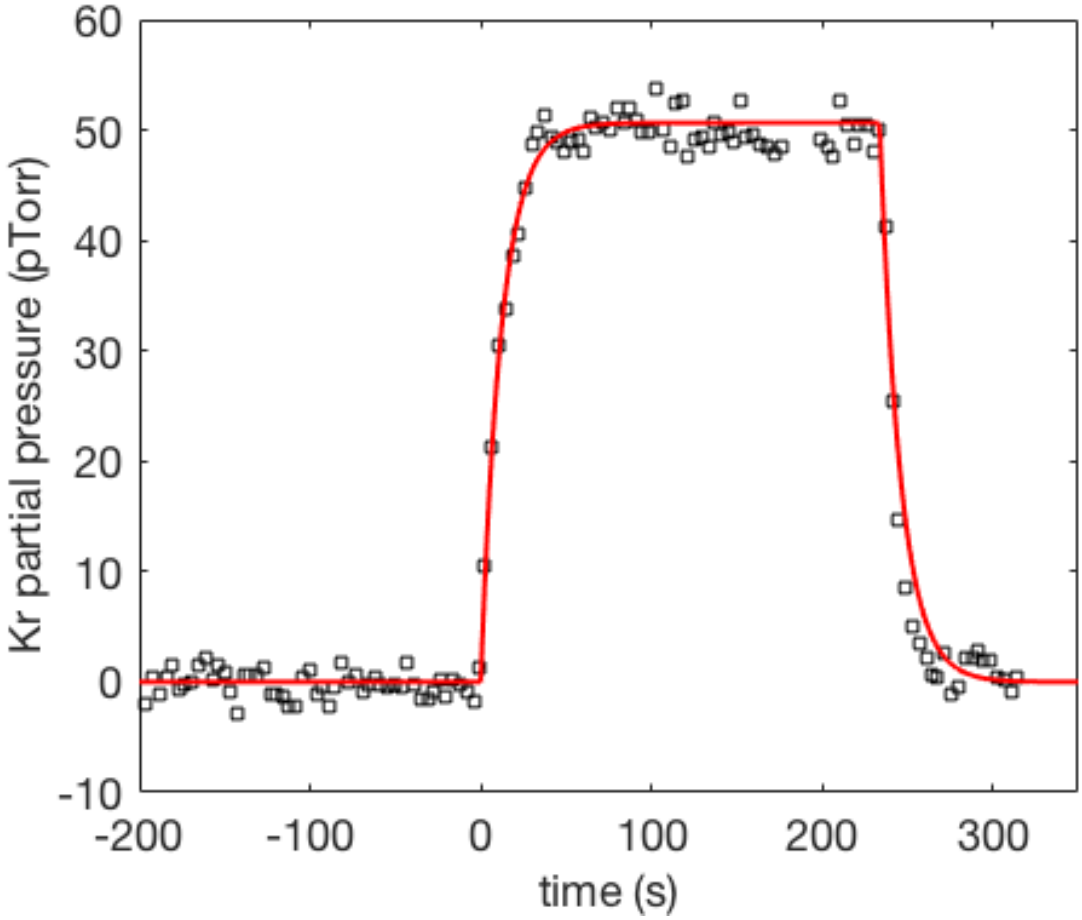

Figure 3: RGA trace with nominal impedance settings. Corrected for RGA gain, the equilibrium pressure of this trace is 50.8 ± 0.4 pTorr. Φ was known to be 750 ± 75 parts per trillion (ppt) in liters of krypton per liter of xenon. The xenon flow rate used was 0.36 standard liters per minute (SLM).

4 Actual Behavior of a Cold Trap System

The vacuum approximation is not perfect, and there are large deviations from the molecular flow model presented in the previous section. These deviations arise from the fact that the cold trap itself is not in equilibrium while the xenon is flowing. The input of the trap has laminar xenon flow where the krypton is interacting primarily gaseous xenon atoms, while at the output of the trap, the xenon is closer to the molecular flow regime, and the krypton atoms will be also interacting with the stainless steel plumbing. More importantly, there is a transition region where the xenon is actively being frozen. This rapid, even violent, phase transition of the xenon has complicated effects on the flow of krypton through the trap, and these effects are found to be dependent upon both the system impedances and the input xenon flow rate.

4.1 Ice Formation

The xenon ice forms in a short segment of plumbing relative to the approximately one foot length of the cold trap. The enthalpy of sublimation for xenon is about 15.95 kJ/mol at 77 kelvin. (*2*). There is an additional 2.73 kJ/mol required to bring the xenon gas temperature down from 295 to 77 kelvin. A 0.36 SLM flow rate is equal to 0.267 mmol/sec of xenon, which requires 5.0 Watts to freeze. If we take the thermal conductance of stainless steel to be 10 W/m K, the maximum cooling power of a 12.7 mm diameter, 1.24 mm thick cold trap will be 70 W/mm.

We must also consider the heat transfer from the LN to the stainless steel trap. The heat transfer rate from LN to a stainless steel surface is highly dependent upon the temperature difference between the bulk LN and the surface. This temperature dependance has a maximum, referred to as the critical heat flux, where the LN changes from “nucleate boiling” to “film boiling”. Film boiling takes place when the LN boils rapidly enough to create an insulating layer, or “film”, of nitrogen gas between the LN bath and the stainless steel surface. The critical

heat flux of Stainless steel to LN is on the order of 10 W/cm^2, putting the maximum heat transfer to our 12.7 mm diameter cold trap at about 4 W/mm, making it the limiting factor in the heat transfer to the plumbing. (*5*)

The above estimates of the heat transfer indicate that at flow rates < 1 SLM, all of the xenon should be frozen within the first centimeter or so of cold plumbing. We can approximately measure the length of the ice-forming region in two ways. First, the length of this region is inferred by observing the bubble formation within the liquid nitrogen bath. As the xenon flow is frozen inside of the trap the heat is transferred to the LN bath, and the nitrogen that is in contact with the ice forming region boils. In order to visually inspect the formation of the ice, we also installed a quartz window on the input and output of a cold trap. At low flow rates (< 1 SLM), both of these methods indicate that the ice formation region is less than about 1 cm in length. When viewing the ice formation through a window, there is a clear collar of xenon ice that forms in the input side of the trap at the level of the LN bath, and there is no visible ice formation anywhere else. When observing the outside of the trap, the LN appears to boil where the plumbing enters the bath but nowhere else.

At higher flow rates (> 1 SLM), the ice no longer forms a collar, but rather a sleeve along the inside of the trap. This is likely due to the xenon ice forming an insulating layer over the stainless steel, thereby reducing the cooling power of that segment of plumbing to the point where it is no longer able to freeze the xenon. In the high flow regime, the LN will still only boil along a short segment of plumbing, but this segment can be seen to migrate along the trap from input to output. Eventually, enough of the trap surface is covered that the trap is no longer able to maintain a constant xenon temperature at the output and the xenon pressure at the RGA rises. This can be contrasted to the behavior at low flow rates, where the xenon collar will eventually grow thick enough to physically clog the trap without the RGA pressures changing at all.

4.2 Krypton Retention: Flow Rate Dependance

As mentioned previously, there are two distinct regimes of xenon flow in a cold trap sampling system: the low flow regime in which all of the xenon ice is formed within millimeters of the LN surface level, and the high flow regime in which the xenon ice forms a sleeve, which eventually can reach the output side of the trap and cause the RGA xenon pressure to rise. In the low flow regime, the response of the sold trap system to flow rate is extremely linear. However, in the high flow regime this linearity breaks down. As the sleeve rounds bends in the trap the krypton pressure at the RGA can be seen to drop from the exponential response predicted in equation 17. It is not clear what the physical cause or causes of this deviation are, but the overall effect is a lower krypton pressure.

4.3 Krypton Retention: Impedance Dependance

Fitting the krypton pressure trace, $P_{Kr,RGA}(t)$ to equation 17 breaks down at high xenon flow rates and high system impedances. We don't know the physical cause of this breakdown, but it is likely tied to the krypton throughput parameter, α, that was introduced in section 3.2. Consider the pressure trace shown in figure 4; the xenon flow rate, Q_0 and krypton concentration, Φ were identical to the krypton trace in figure 3, and the impedance, Z_1 was set to be 45 time higher. This trace deviates significantly from what would be expected by increasing Z_1 in equation **??**. Both the system response time and equilibrium pressure are expected to increase proportional to Z_1 from equations 14 and 10, but had a significantly smaller increase. $PP_{Kr,eq}$ increased from 50.8 ± 0.4 to 399.9 ± 1.7 pTorr; a factor of 7.9. The overall response time, τ, increased from 12.7 ± 0.7 to 93.4 ± 1.8 seconds; a factor of 7.4.

Although $PP_{Kr,eq}$ and τ no not remain proportional to Z_1, they do remain proportional to each other.

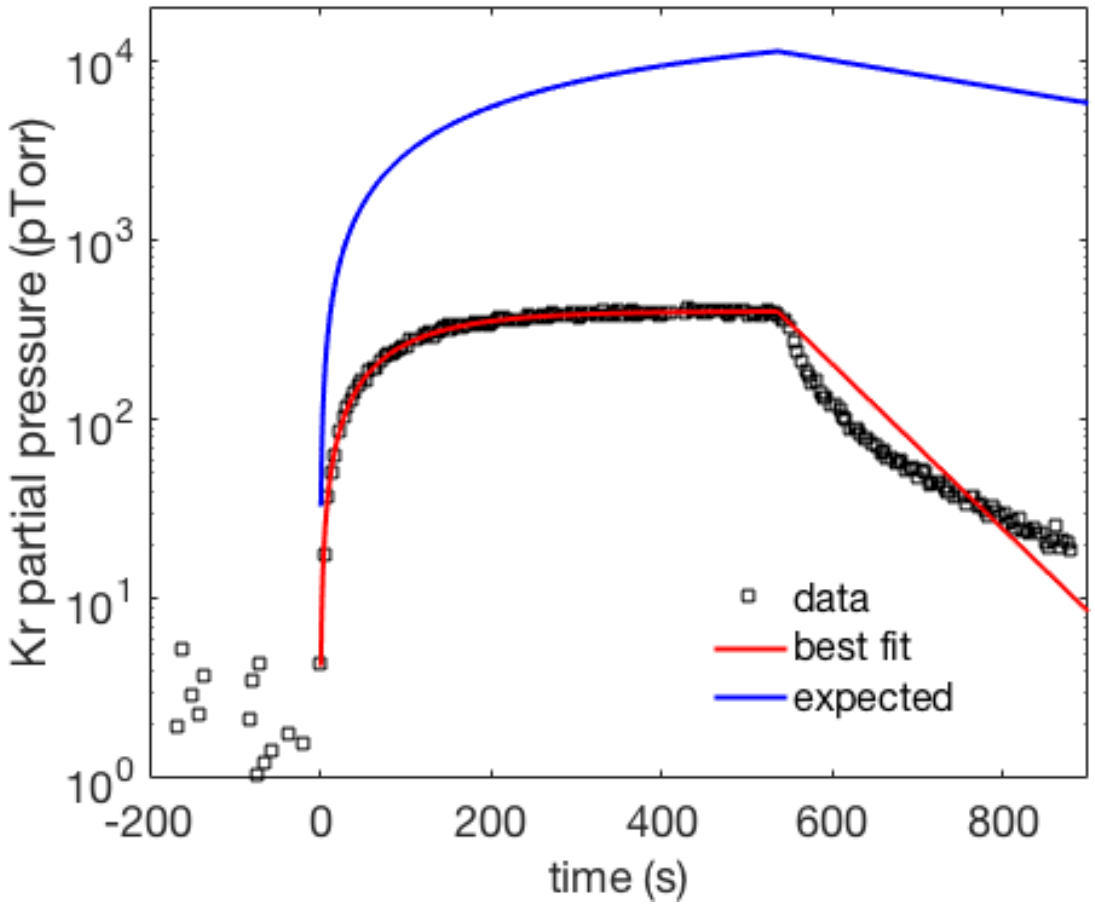

Figure 4: RGA trace with 45x impedance settings.

5 Analysis Scheme

The physical value we are interested in measuring is the concentration of an impurity, specifically krypton, in a sample of xenon gas. This value is typically referred to as Φ and cited in units of grams of krypton per gram of xenon. The calculation of Φ is done using the RGA partial pressure data collected between steps 3 and 7 of the procedure outlined in section 2.2. An example of this data is shown in figure 5.

There are four distinct time-intervals in figure 5 labelled I through IV.

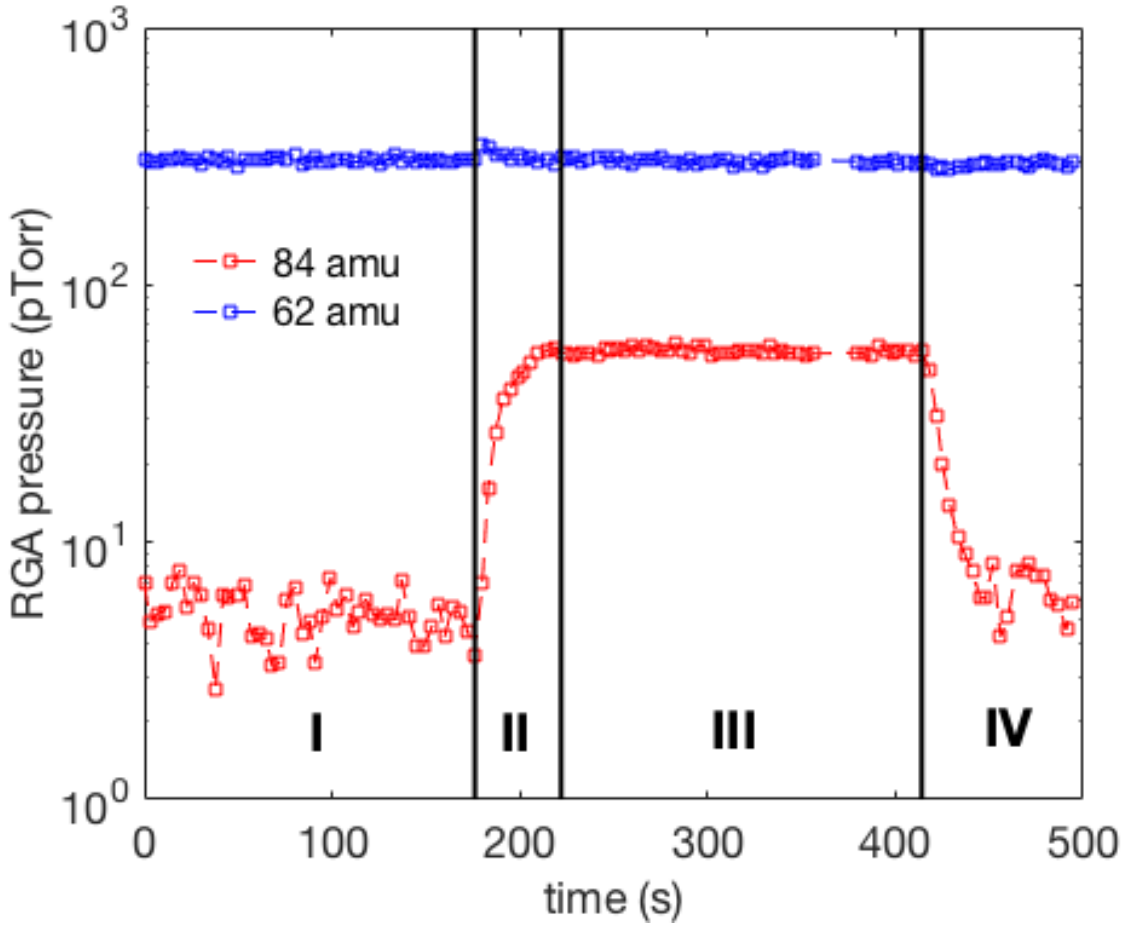

Figure 5: The RGA-measured partial pressures of the 84 amu krypton peak and doubly ionized Xe-124 which appears as a peak at 62 amu. The four time intervals indicate: static baseline, rising Kr trace, steady-state Kr pressure, and post-flow Kr pressure fall.

- I is the period of time after ice has been formed (step 3), but before the xenon flow has been started (step 5). During this interval, both xenon and krypton traces should be constant; if they are trending or otherwise varying systematically, there is some problem that needs to be addressed before continuing. The average krypton pressure over this interval is used as the baseline value and will be subtracted from the analysis pressure. The average xenon pressure can be used as a measure of the RGA gain, since the physical xenon pressure will not change between sample analyses.

- II is the period of time after xenon flow has been started (step 5), but before the krypton pressure has reached its equilibrium value. Given a long enough cold trap the krypton pressure during this step would fit a 1-exponential model, but the geometry of the cold trap can cause kinks in the trace. It is common for there to be a small transient effect in the xenon pressure as is seen here. This is likely due to the ice temperature increasing due to the added heat load from the flowing xenon. This transient effect can illicit an electronic response in the RGA baseline pressure which will mimmic a small krypton signal. The mitigation of this effect will be described in a later section.

- III is the period of time during which the krypton pressure is at its equilibrium value. This equilibrium pressure is determined by the flow rate of the xenon, the sensitivity of the system, and Φ.

- IV is the period of time after the xenon flow has been stopped (step 6). During this period the krypton pressure will fall away exponentially before it eventually returns to the baseline value.

When the flow of krypton has equilibrated throughout the system, Φ can be related to the flow rate and RGA krypton partial pressure through the following equation:

$$\Phi = \frac{P_{Kr,RGA}}{CQ_{Xe,CT}}, \tag{19}$$

where C is a calibration constant which encapsulates the sensitivity of the system, $Q_{Xe,CT}$ is the instantaneous flow rate of xenon into the cold trap, and $P_{Kr,RGA}$ is the krypton pressure. It is possible that there is a physical background seen by the RGA at the mass of interest (84 amu for the case of krypton), but we are only interested in the pressure which is extracted from the xenon sample. To account for any non-zero baseline we subtract out $\overline{PP}_{Kr,0}$, the average krypton pressure measured by the RGA during region I.

When paired with a concurrent flow-rate measurement, $Q_{Xe,i}$, each RGA data point, $PP_{Kr,i}$, collected in region III will give an individual measurement of the purity of the xenon sample, ϕ_i:

$$\phi_i = \frac{1}{C}\frac{PP_{Kr,i} - \overline{PP}_{Kr,0}}{Q_{Xe,i}}. \tag{20}$$

We take the average of these individual purity measurements as the final result of the analysis:

$$\Phi = \overline{\phi_i}, \tag{21}$$

with N being the number of RGA data points collected in region III. The random uncertainty on this purity result is taken to be the standard error:

$$\sigma_\Phi = \frac{\sigma\phi}{\sqrt{N}}, \tag{22}$$

where σ_ϕ is the standard deviation of the collection of ϕ_i's. This method of analysis has been previously shown to be linear with purity. (*3, 4, 6*)

In order to maximize the krypton sensitivity, we operate in a high-impedance mode (described in later sections) which increases the rise and fall time of the krypton pressure. This being the case, we wish to allow $PP_{Kr,i}$ to be drawn from the non-equilibrium regions II and IV, as well as region III. This In these cases we assume a more general version of equation 19:

$$P_{Kr,RGA}(t) = C\Phi f_Q(t), \tag{23}$$

where $f_Q(t)$ is some function which defines the shape of the krypton pressure trace, given a specific flow rate profile, $Q_{Xe,CT}(t)$. $\Phi f_Q(t)$ represents the flow of krypton out of the cold trap, $Q_{Kr,RGA}(t)$, and can be thought of as the input krypton flow, $Q_{Kr,CT} = \Phi Q_{Xe,CT}$, modified by the response of the system. Equation 23 will be valid as long as the response is linear with concentration. For example, consider the krypton trace shown in figure 5. The flow rate profile for this trace is:

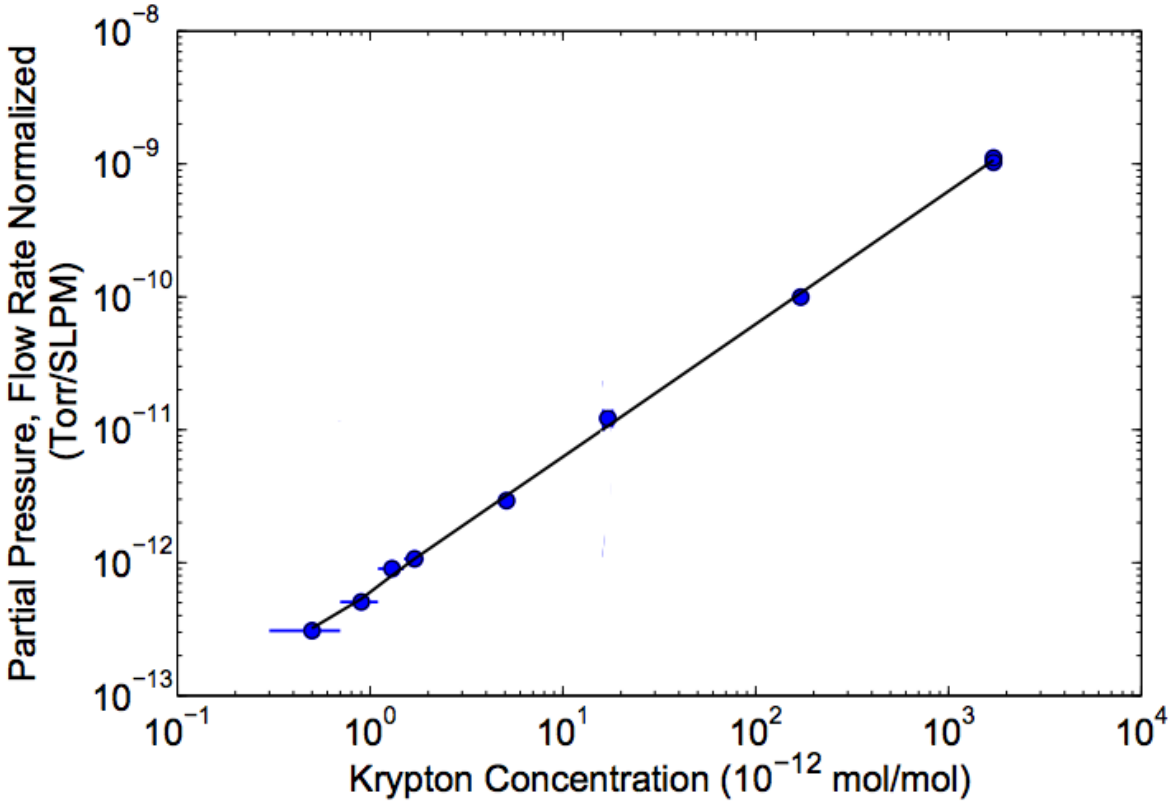

Figure 6: The linearity of the averaging analysis method. The slope of this line will be equal to the calibration constant, C. (*4*)

In section 3 we find that an ideal system is expected to have an exponential response to flow. Convolving equation 16 with an exponential response yields the following shape function

$$f_Q(t) = Q_0 \begin{cases} 0 & \text{for } t \text{ in region I} \\ 1 - \exp(-\frac{t-t_1}{\tau}) & \text{for } t \text{ in region II or III} \\ \exp(-\frac{t-t_2}{\tau}) & \text{for } t \text{ in region IV} \end{cases} \tag{24}$$

Fitting this shape function to the data in figure 5 gives $\tau = 11.6$ seconds. It should be noted here that the pressure trace shown in figure 7a does not fit this shape. This is because the response of the system to flow becomes non-linear at high flow rate and high impedances. Figure 7b shows that response does remain linear in concentration even when it is not linear in flow.

We now integrate equation 23 between some t_1 and t_2:

$$\int_{t_1}^{t_2} P_{Kr,RGA} dt = \Phi F_{Q,t_1,t_2}, \tag{25}$$

where:

$$F_{Q,t_1,t_2} \equiv \int_{t_1}^{t_2} f_Q(t) dt. \tag{26}$$

In terms of the discrete RGA measurements, $PP_{Kr,i}$ this becomes:

$$\Phi = \frac{1}{F_{Q,t_1,t_2} C} \sum_{i=1}^{N} (PP_{Kr,i} - \overline{PP}_{Kr,0}) \Delta t_i. \tag{27}$$

$F_{Q,t_1,t_2}C$ is a constant of proportionality which can be measured by analyzing a xenon sample with a known Φ. However, this constant will only hold so long as $Q_{Xe,CT}(t)$, t_1, and t_2 are identical between the analysis and calibration runs. To ensure consistency, it is best practice to calibrate after every sample analysis. These calibrations should follow the procedure described in section **??** and should use the left-over sample xenon which is recovered from the cold trap as the base "clean" xenon. This can be done as long as the initial concentration of krypton in the xenon sample is much less than the target concentration of the calibration xenon.

The random uncertainty of purity results calculated using equation 27 are harder to estimate than those calculated using equation 21. The fluctuations around each datapoint cannot be measured directly, so they are estimated using the baseline data collected in region I. The fluctuations of the RGA tend to increase at higher partial pressure, as shown in figure 8. We take the baseline fluctuations, σ_0, to be equal to the standard deviation of the region I data points. The random uncertainty of each data point, $PP_{Kr,i}$, is then taken to be:

$$\sigma_i = \sigma_0 * (1 + 0.009 * PP_{Kr,i}). \tag{28}$$

The propagation of this error to Φ is then:

$$\sigma_\Phi^2 = \frac{1}{F_{Q,t_1,t_2}^2 C^2} \sum_{i=1}^{N} (\sigma_i^2 + \sigma_0^2/N_B) \Delta t_i, \tag{29}$$

where N_B is the number of data points used in the calculation of $\overline{PP}_{Kr,0}$ and σ_0.

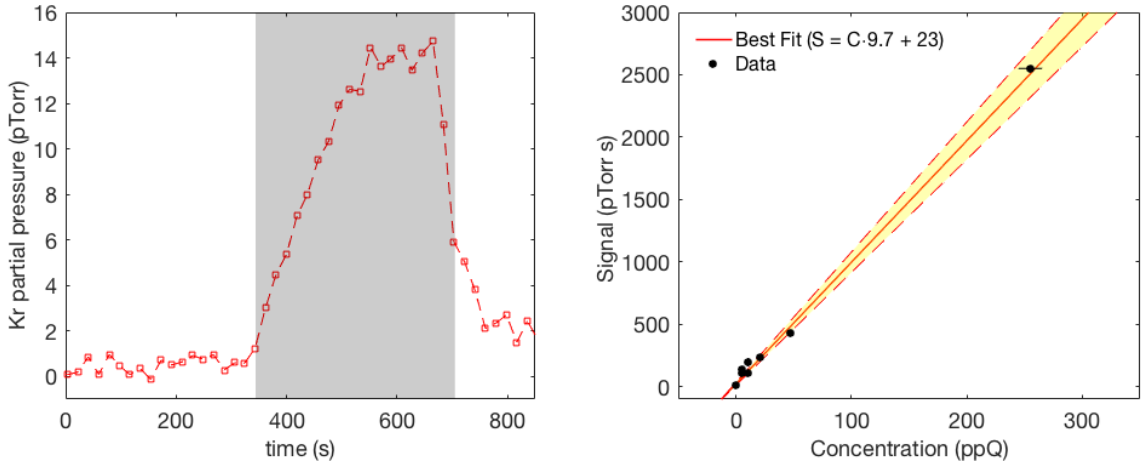

(a) Sample RGA trace.

(b) Linearity of analysis.

Figure 7: Linearity of the integration-style analysis described in equation 27. The krypton signals used in these measurements never reached an equilibrium value. The xenon flow profile for theses measurements was a square pulse. The height of this pulse was set using an MFC, and the time-width of the pulse was defined by the size of the xenon sample used. t_1 was defined as the start of the xenon flow, plus 20 seconds, and t_2 was defined as the stop of the xenon flow, plus 20 seconds.

6 System Parameters and Optimization

Optimizing a cold-trap sampling system is a matter of maximizing the signal to noise ratio, which comes down to minimizing the fluctuations in the RGA baseline and maximizing the system response to krypton. There are several knobs and dials to turn to achieve this, but adjusting one of the knobs might change how one of the dials affects the sensitivity. This section will attempt to catalog the affect of these adjustments in an empirical way and will describe the optimal arrangement.

6.1 RGA Parameters

The first and simplest adjustments to be made are to the RGA electronics. These adjustments can be made quickly and easily, and are largely independent from the other knobs and dials.

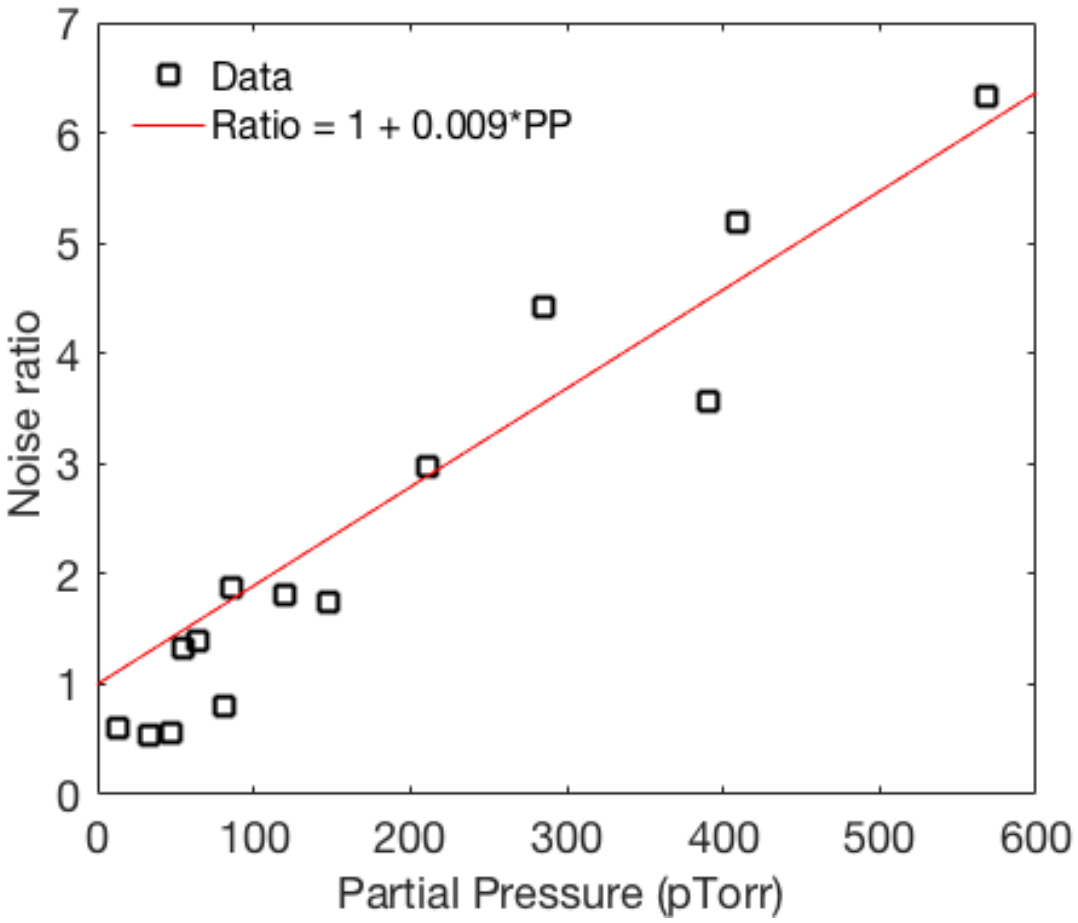

Figure 8: The trend in RGA fluctuations as a function of partial pressure. The noise ratio is defined as the fraction by which the RGA fluctuations increase when the partial pressure is increased from its baseline value (Noise ratio $\equiv \sigma(PP)/\sigma(baseline)$).

There is a long list of internal RGA parameters which should be understood before operating a cold trap system. These can be found in chapter 6 of the RGA manual. The two parameters that have the greatest effect on the sensitivity to krypton are the noise floor and the high-voltage setting of the continuous dynode electron multiplier (CDEM).

The noise floor sets the scan speed of the RGA; the lower the noise floor setting, the longer the RGA will spend integrating current on a single mass point. The practical effects are three-fold. The obvious first implication is that with a low noise floor, it will take much longer to to

collect a single data point. At a noise floor setting of 0 the RGA will sit on a mass point for more than 5 seconds, and at a noise floor setting of 3 it will sit for less than 0.5 seconds per mass. For high-sensitivity analysis, it is better to have the noise floor set as low as possible, which will give you fewer data points which have a smaller variance. This will reduce the amount of time spent communicating with the RGA, as well as the amount of down time between communications.

At higher noise floors, there tends to be an offset in the baseline. While we usually try to account for this by using baseline-subtracted pressures in purity calculations, it is possible that the shifted baseline is not additive to the pressure signal. This is indicated by the krypton signal in the LUX run04 data decreasing artificially. There is also evidence from the SLAC system that the baseline is not strictly additive to a physical pressure signal.

Setting the voltage on the CDEM is a balancing act. Increasing the voltage increased the signal amplification. Above a certain CDEM voltage, however, the random fluctuations in the RGA baseline rise faster than the gain, and if the voltage is set too high, the xenon ice vapor pressure will begin saturate the CDEM, degrading and possibly damaging it. The CDEM voltage should be high enough that the largest xenon peaks such as 132 and 133 should be at saturation but not so high that the doubly ionized peaks such as 66 amu saturate.

The health of the CDEM can be tracked using one of the xenon ice peaks, assuming the MG and SP parameters are not changed. MG is the CDEM gain factor and SP is the mass sensitivity factor used to convert the RGA current to partial pressure. The physical values may change over time, but the parameter stored in the RGA memory will not change unless a head-calibration is run. In particular, as the CDEM degrades, the gain will fall. A drift in the gain will bee seen most easily as a drop in the measured xenon ice pressure. Since the vapor pressure of xenon ice at 77 Kelvin is physically constant, if this pressure reading drops, it indicates that the gain has dropped. To maintain the CDEM gain, the xenon peak at 62 amu should be monitored. Whenever this value drops, the voltage should be increased until the pressure returns to its initial

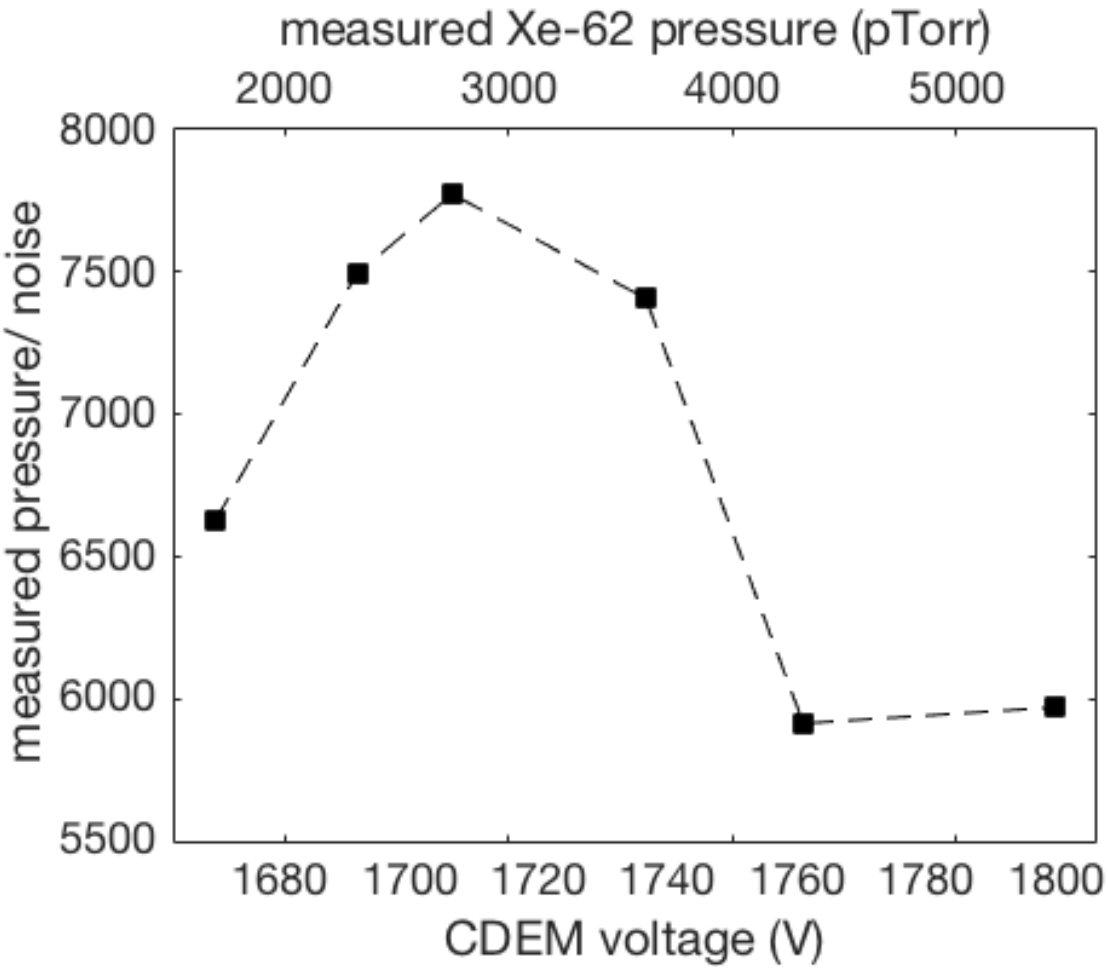

Figure 9: RGA sensitivity as a function of CDEM voltage.

value.

6.2 Flow Rate

Consider the idealized pressure trace shown in figure 11, which is the result of a rectangular flow rate profile into a system which has an instantaneous response. The flat top of this trace will have a height of $PP_{Kr,eq} = C$. The width of this pulse will be given by the amount of xenon used in the analysis ($V\Delta P$) divided by the flow rate of the xenon into the cold trap $Q_{Xe,CT}$. Both the averaging method from equation 21, and the integration method from equation 27

would give a signal-to-noise proportional to $1/\sqrt{N}$, with N being the number of data points in the top of the square pulse. Using a constant RGA sampling rate of r we find that the expression for signal to noise in either case will be:

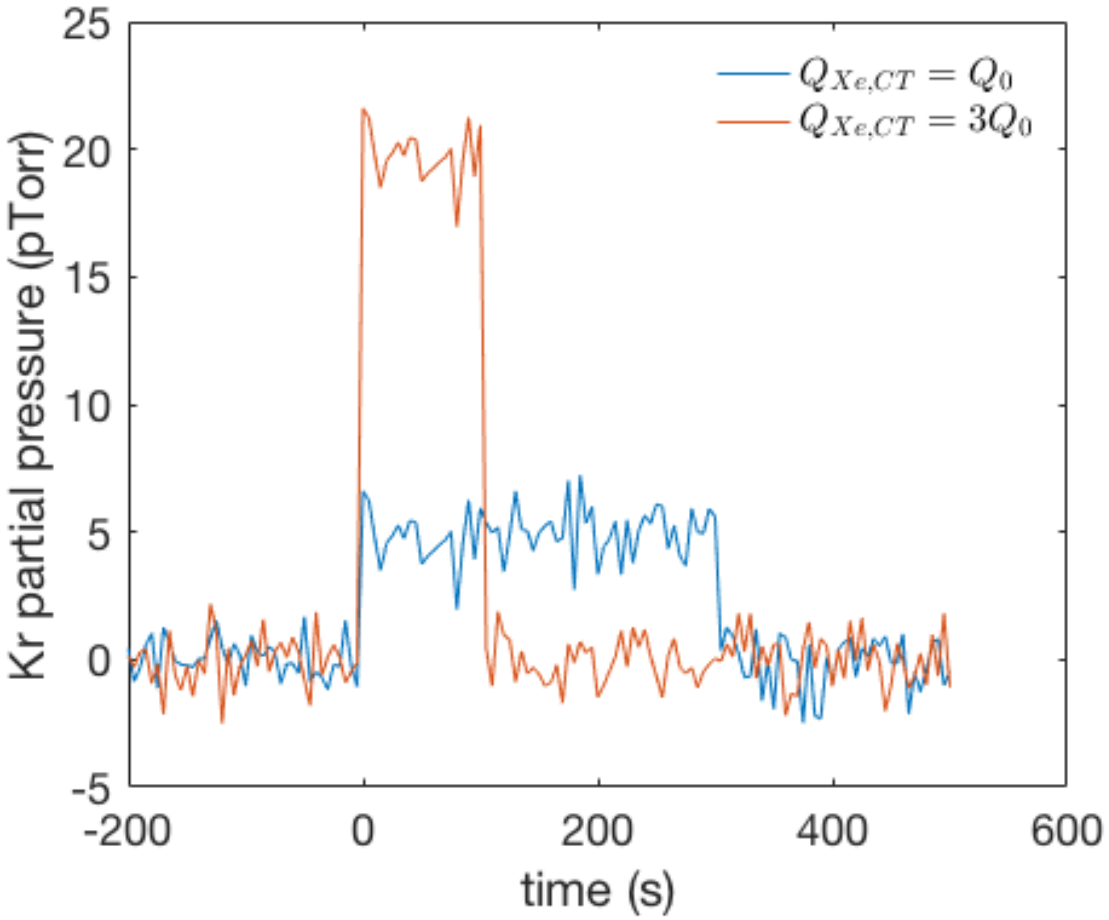

Figure 10: Peak krypton RGA pressure as a function of flow rate.

6.3 Impedance

With the RGA sensitivity optimized, we now aim to maximize the krypton pressure which it is attempting to measure. To this end, we return to equation 10, which indicates that in addition

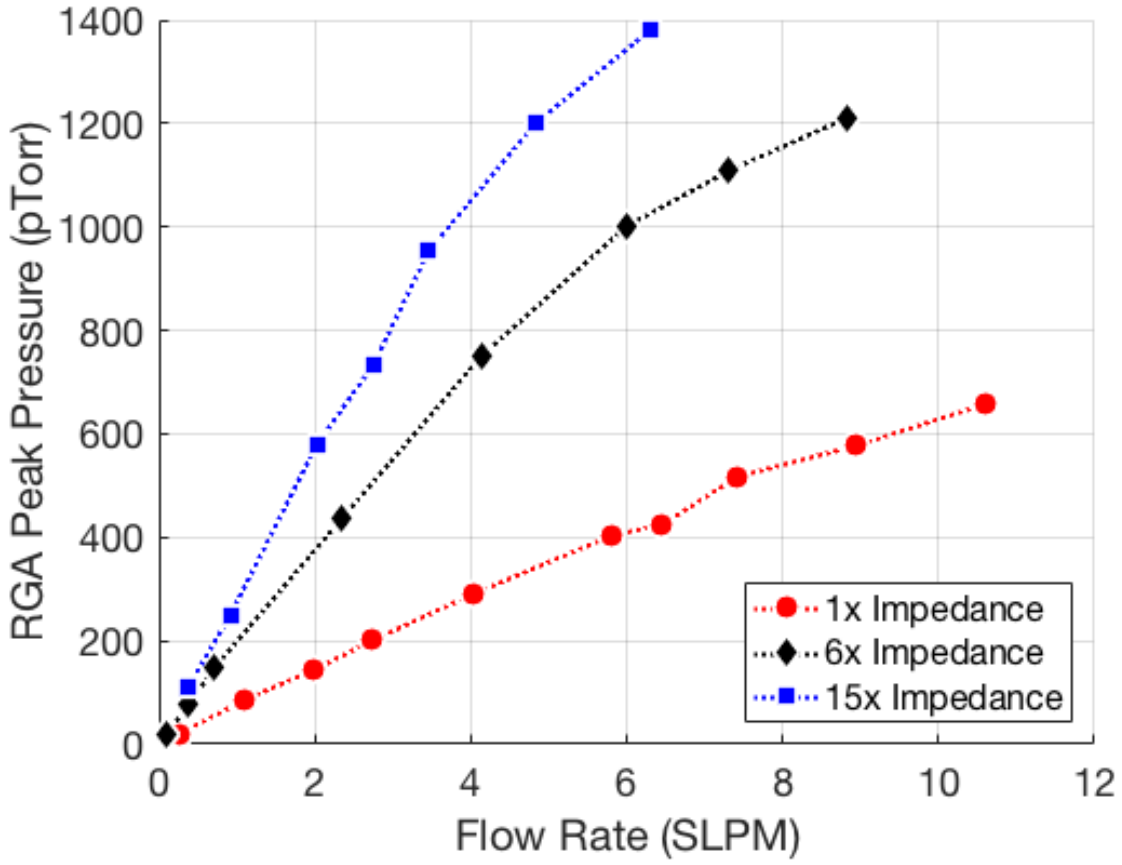

Figure 11: Peak krypton RGA pressure as a function of flow rate.

6.4 System Geometry

6.5 Ice Formation Procedure

7 Calibrations

Once the system has been optimized using a largely arbitrary mixture of xenon and krypton, the next key step is to measure the response of the system to a series of mixtures referred to as calibration xenon which have well known concentrations of krypton. Once this response is known, the system can be used to measure concentrations of unknown mixtures. To this end, the preparation of a mixture of xenon and krypton with a well known concentration is essential.

7.1 Preparation of Calibration Xenon

The first ingredient in the preparation of this mixture is extremely pure xenon. This is obtained by using the cold trap system itself to clean a small amount of stock xenon. As was explained previously, the cold trap analysis works because all but a microscopic amount of xenon is retained by the cold trap, while gasses such as krypton pass through largely unaffected. This means that the xenon that remains in the cold trap after an analysis has significantly lower krypton content than before the analysis. Depending on the system parameters, the post-run xenon will contain as little as $1/15^{\text{th}}$ the krypton as the pre-run xenon. Using the system described by figure **??**, it takes about 3 hours to purify 100g of typical stock xenon with a concentration of 1 part in 10^9 down to < 1 part in 10^{15},

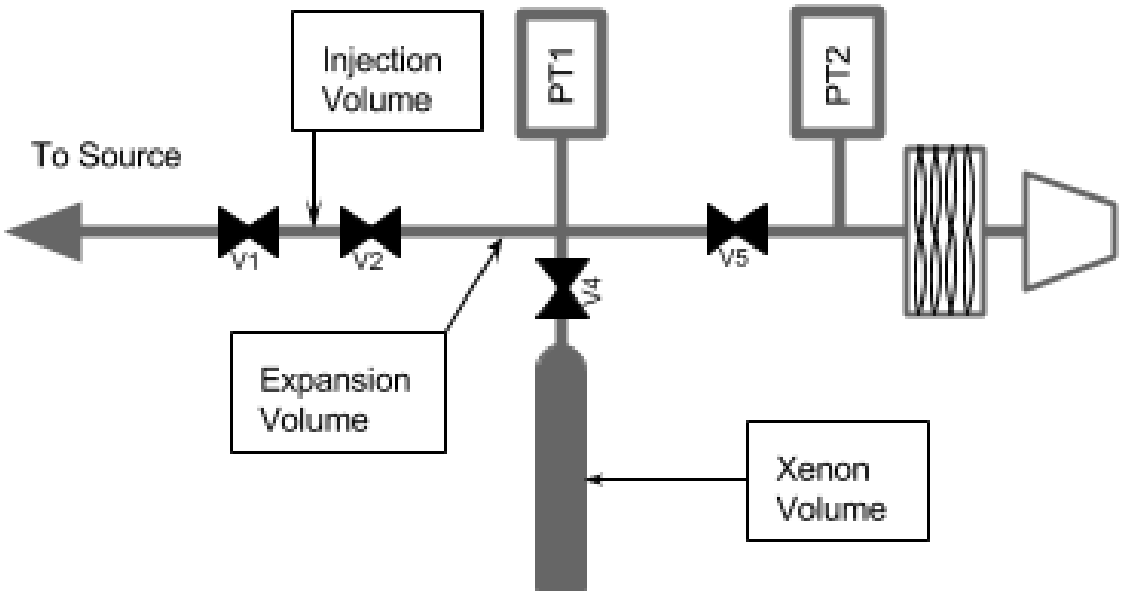

Figure 12: Plumbing diagram of a generalized mixing system.

Once the xenon has been cleaned it is transferred to an appropriate mixing system, described by figure 12. The relative volumes of this system must be extremely well known, so they are measured using volume sharing. First the full system, including injection, expansion, and xenon

volumes, is filled with roughly 2000 torr of xenon as measured by pressure transducer 1. Then the expansion volume is pumped to vacuum, leaving a well known pressure in both the injection and xenon volumes. Valve 4 is opened to expose the xenon within the xenon volume to the expansion volume. The resulting pressure on PT1 gives the expansion volume relative to the xenon volume. Through the ideal gas law, when temperature is constant and mass is conserved, pressure times volume will remain constant:

$$P_1 V_1 = P_2 V_2 \tag{30}$$

Therefore, the size of the expansion volume relative to the xenon volume can be calculated using:

$$\frac{\text{Expansion Vol.}}{\text{Xenon Vol.}} = P_1/P_2 - 1. \tag{31}$$

Similarly, the relative size of the injection volume is found by expanding the known pressure within the injection volume into the expansion volume.

To prepare the calibration xenon, the injection volume is filled to some known pressure with pure krypton. The krypton is then opened to the expansion volume in order to reduce the pressure, and then the expansion volume is pumped out using a the turbo-pump until PT2 reads $< 1 \times 10^{-6}$ torr. This expansion is repeated until the desired krypton pressure is reached. After the final expansion volume pump-out, the xenon volume is opened to the injection volume, and the new xenon/krypton mixture is frozen back into the xenon volume using liquid nitrogen. The krypton concentration (Φ_{Kr}) of the calibration xenon in grams krypton per grams xenon is given by:

$$\Phi_{Kr} = \frac{\alpha^N P_{Kr}(\text{Injection Vol.})\rho_{Kr}}{P_{Xe}(\text{Xenon Vol.})\rho_{Xe}}, \tag{32}$$

where the expansion ration, α, is given by (Injection Vol.)/(Injection Vol. + Expansion Vol.), N is the number of expansions, P_{Kr} and P_{Xe} are the krypton and xenon pressures initially injected into the system, and ρ_{Kr} and ρ_{Xe} are the krypton and xenon gas densities.

The injection pressure must be kept above 0.01 torr to ensure the krypton remains above the molecular flow regime. This sets a lower limit on the concentration of calibration xenon that can be produced through this method. With an injection volume of 5cc and a xenon volume of 4000cc, the lowest concentration than can be produced from pure krypton is about 5 PPB. In order to produce calibration xenon with smaller concentrations, the pure krypton is replaced with the PPB level calibration xenon, which is diluted into clean xenon through the same process outlined in the previous paragraph.

7.2 Calibration Procedure

8 Sensitivity Demonstration

A Sample Procedures

References and Notes

1. N. Marquardt (1999).

2. A. Ferreira, L. Lobo, *The Journal of Chemical Thermodynamics* **40**, 1621 (2008).

3. D. S. Leonard, *et al.*, *Nucl. Instrum. Meth.* **A621**, 678 (2010).

4. A. Dobi, *et al.*, *Nucl. Instrum. Meth.* **A665**, 1 (2011).

5. E. Roth, Nucleation and heat transfer in liquid nitrogen, Ph.D. thesis, Portland State University (1993).

6. A. Dobi, *et al.*, *Nucl. Instrum. Meth.* **A675**, 40 (2012).